Research Article | Vol. 25, No. 24 | 27 Nov 2017 | OPTICS EXPRESS 29587
Optics EXPRESS

8-beam local oscillator array at 4.7 THz generated by a phase grating and a quantum cascade laser

B. Mirzaei,[1] J. R. G. Silva,[2] D. Hayton,[2] C. Groppi,[3] T. Y. Kao,[4] Q. Hu,[4] J. L. Reno,[5] and J. R. Gao[1,2]

[1]*Kavli Institute of Nanoscience, Delft University of Technology, Lorentzweg 1, 2628 CJ, Delft, The Netherlands*
[2]*SRON Netherlands Institute for Space Research, Sorbonnelaan 2, 3584 CA Utrecht, The Netherlands*
[3]*School of Earth and Space Exploration, Arizona State University, AZ, USA*
[4]*Department of Electrical Engineering and Computer Science, Massachusetts Institute of Technology (MIT), Cambridge, Massachusetts 02139, USA*
[5]*Center for Integrated Nanotechnologies, Sandia National Laboratories, Albuquerque, NM 87185-0601, USA*
[6]*b.mirzaei@tudelft.nl*
[7]*j.r.gao@tudelft.nl*

Abstract: We present an 8-beam local oscillator (LO) for the astronomically significant [OI] line at 4.7 THz. The beams are generated using a quantum cascade laser (QCL) in combination with a Fourier phase grating. The grating is fully characterized using a third order distributed feedback (DFB) QCL with a single mode emission at 4.7 THz as the input. The measured diffraction efficiency of 74.3% is in an excellent agreement with the calculated result of 75.4% using a 3D simulation. We show that the power distribution among the diffracted beams is uniform enough for pumping an array receiver. To validate the grating bandwidth, we apply a far-infrared (FIR) gas laser emission at 5.3 THz as the input and find a very similar performance in terms of efficiency, power distribution, and spatial configuration of the diffracted beams. Both results represent the highest operating frequencies of THz phase gratings reported in the literature. By injecting one of the eight diffracted 4.7 THz beams into a superconducting hot electron bolometer (HEB) mixer, we find that the coupled power, taking the optical loss into account, is in consistency with the QCL power value.

OCIS codes: (050.1950) Diffraction gratings; (140.5965) Semiconductor lasers, quantum cascade; (040.2840) Heterodyne; (040.2235) Far infrared or terahertz; (040.1240) Arrays; (350.1260) Astronomical optics.

References and links

1. C. Kulesa, "Terahertz spectroscopy for astronomy: from comets to cosmology," IEEE Trans. THz. Sci. Tech. (Paris) **1**, 232–240 (2011).
2. C. Walker, Terahertz Astronomy (CRC, Taylor & Francis Group, 2016), Chap. 5 and 6.
3. J. V. Siles, R. H. Lin, C. Lee, E. Schlecht, A. Maestrini, P. Bruneau, A. Peralta, J. Kloosterman, J. Kawamura, and I. Mehdi, "Development of high-power multi-pixel LO sources at 1.47 THz and 1.9 THz for astrophysics: present and future," in *Proceedings of the 26th International Symposium on Space Terahertz Technology* (Cambridge, MA, 2015), pp. 40–42.
4. C. Groppi, C. Walker, C. Kulesa, D. Golish, J. Kloosterman, S. Weinreb, G. Jones, J. Barden, H. Mani, T. Kuiper, J. Kooi, A. Lichtenberger, T. Cecil, and G. Narayanan, P. Pu˙tz and A. Hedden, "SuperCam: A 64 pixel heterodyne array receiver for the 350 GHz atmospheric window," in *Proceedings of the 20th International Symposium on Space Terahertz Technology* (Charlottesville, 2009), pp. 90–96.
5. J. A. Murphy, C. O. Sullivan, N. Trappe, W. Lanigan, R. Colgan, and S. Wittington, "Modal Analysis of the Quasi-Optical Performance of Phase Gratings," Int. J. Inf Mill. Waves **20**, 1469–1486 (1999).
6. U. U. Garf and S. Heyminck, "Fourier gratings as submillimeter beam splitters," IEEE Trans. Antenn. Propag. **49**, 542–546 (2001).
7. A. G. G. M. Tielens and D. Hollenbach, "Photodissociation regions. I. basic model. II. A model for the Orion photodissociation Region," Astrophys. J. **291**, 722–754 (1985).

#303729 https://doi.org/10.1364/OE.25.029587
Journal © 2017 Received 1 Aug 2017; revised 16 Oct 2017; accepted 16 Oct 2017; published 13 Nov 2017

Optics EXPRESS

8. S. Leurini, F. Wyrowski, H. Wiesemeyer, A. Gusdorf, R. Gusten, K. M. Menten, M. Gerin, F. Levrier, H. W. Hubers, K. Jacobs, O. Ricken, and H. Richter, "Spectroscopically resolved far-IR observations of the massive star-forming region G5.89-0.39," Astron. Astrophys. **584**, A70 (2015).
9. B. S. Williams, "Terahertz quantum-cascade lasers," Nat. Photonics **1**, 517–525 (2007).
10. M. I. Amanti, G. Scalari, F. Castellano, M. Beck, and J. Faist, "Low divergence Terahertz photonic-wire laser," Opt. Express **18**(6), 6390–6395 (2010).
11. B. Mirzaei, J. R. G. Silva, Y. C. Luo, X. X. Liu, L. Wei, D. J. Hayton, J. R. Gao, and C. Groppi, "Efficiency of multi-beam Fourier phase gratings at 1.4 THz," Opt. Express **25**(6), 6581–6588 (2017).
12. M. Cui, J. N. Hovenier, Y. Ren, N. Vercruyssen, J. R. Gao, T. Y. Kao, Q. Hu, and J. L. Reno, "Beam and phase distributions of a terahertz quantum cascade wire laser," Appl. Phys. Lett. **102**, 111113 (2013).
13. W. C. Elmore and M. A. Heald, *Physics of waves* (Dover Publications, Inc., New York, 1969).
14. H. Ehrenreich, H. R. Philipp, and B. Segall, "Optical properties of aluminum," Phys. Rev. **132**, 1918–1928 (1963).
15. B. S. Williams, S. Kumar, Q. Hu, and J. L. Reno, "Resonant phonon terahertz quantum-cascade laser operating at 2.1 THz ($\lambda \approx 141$ μm)," Electron. Lett. **40**, 431–433 (2004).
16. J. L. Kloosterman, D. J. Hayton, Y. Ren, T. Y. Kao, J. N. Hovenier, J. R. Gao, T. M. Klapwijk, Q. Hu, C. K. Walker, and J. L. Reno, "Hot electron bolometer heterodyne receiver with a 4.7-THz quantum cascade laser as a local oscillator," Appl. Phys. Lett. **102**, 011123 (2013).
17. W. Zhang, P. Khosropanah, J. R. Gao, T. Bansal, T. M. Klapwijk, W. Miao, and S. C. Shi, "Noise temperature and beam pattern of an NbN hot electron bolometer mixer at 5.25 THz," J. Appl. Phys. **108**, 093102 (2010).
18. H. Ekström, B. S. Karasik, E. Kollberg, and K. S. Yngvesson, "Conversion gain and noise of niobium superconducting hot-electron-mixers," IEEE Trans. Microw. Theory Tech. **43**, 938–947 (1995).
19. L. P. Boivin, "Multiple Imaging Using Various Types of Simple Phase Gratings," Appl. Opt. **11**(8), 1782–1792 (1972).
20. The quoted optical loss is contributed by the HEB-antenna coupling (0.5 dB), the spiral antenna (3 dB, for a linearly polarized Gaussian beam), the Si lens reflection loss (1.2 dB), the QMC heat filter (0.4 dB), the HEB cryostat UHMW-PE window (1.4 dB), the HDPE focusing lens (1.2 dB), the air loss (1 dB), the phase grating (10 dB), the beam stop (in combination with two mirrors) (12.5 dB), and the UHMW-PE window of the QCL cryostat (1.4 dB).
21. The quoted optical loss is contributed by the HEB-antenna coupling (0.5 dB), the spiral antenna (3 dB, for a linearly polarized Gaussian beam), the AR coated Si lens reflection loss (0.15 dB), the QMC heat filter (0.4 dB), the HEB cryostat UHMW-PE window (1.4 dB), the Si focusing lens with AR coating on both sides (0.3 dB), the phase grating (10 dB), the beam splitter (9 dB), and the UHMW-PE window of the QCL cryostat (1.4 dB).
22. T. Y. Kao, X. Cai, A. W. M. Lee, J. L. Reno, and Q. Hu, "Antenna coupled photonic wire lasers," Opt. Express **23**(13), 17091–17100 (2015).
23. A. Khalatpour, J. L. Reno, N. P. Kherani, and Q. Hu, "Unidirectional photonic wire laser," Nat. Photonics **11**, 555–559 (2017).

1. Introduction

Heterodyne spectroscopy provides valuable scientific information for modern astrophysics, in particular, the process of star formation and the life cycle of interstellar clouds in our own and nearby galaxies. It has the capability to measure molecular and atomic fine structure lines in the super-terahertz frequency region (> 1 THz) [1] including ionized nitrogen [NII] at 1.4 THz, ionized carbon [CII] at 1.9 THz, hydrogen deuteride [HD] at 2.6 THz and neutral oxygen [OI] at 4.7 THz, each containing unique source of information. One important observation is to map particular THz lines in star forming areas within our Milky Way at very high spectral resolution. Such large-scale surveys with velocity-resolved imaging of key fine structure lines require multi-pixel heterodyne receivers [2] with the state-of-the-art mixer performance in order to increase the observation speed and thus the observing efficiency of the telescope. A single heterodyne receiver with extremely high spectral resolving power of 10^6-10^7, consists typically of a mixing detector, a local oscillator (LO), a low noise GHz cryogenic amplifier and a backend GHz spectrometer. Because of the complexity of the receiver and especially the power dissipation of low noise cryogenic amplifiers, the state-of-the-art heterodyne receiver arrays typically have in the order of 10 pixels. Furthermore, very few instruments using multi-pixel receivers have been demonstrated at THz frequencies in the literature.

A multi-pixel heterodyne receiver therefore requires multiple parallel receivers; each pumped with its own LO beam. In general, advanced fabrication technology allows making relatively uniform array of mixers, so that (as will be shown later in this paper) within a

Optics EXPRESS

certain variation of the LO power they still deliver receiver sensitivities with negligible differences. For generating multiple THz LO beams two approaches have been reported: solid-state waveguide multiple beam generators based on frequency multipliers driven by a common microwave source [3,4], and reflective phase gratings for generating multiple beams by diffracting a single THz source [5,6]. A phase grating is a periodic arrangement of a unit cell with a specific surface morphology for phase manipulation of the incident coherent radiation. Such a surface profile determines the intensity distribution among the diffracted beams, their angular configuration, and the diffraction efficiency. The latter is defined as the ratio of the total power of the desired diffraction orders to the power of the incoming beam. We will call it efficiency in the rest of the paper.

The choice of the LO technologies depends strongly on the frequency. The neutral oxygen [OI] line at 4.7 THz mostly probes warm natural gas heated by massive newly formed stars [7,8]. As such, it is useful for probing the star formation process, especially when the emission is spectrally resolved. However, because the technology at this frequency is not sufficiently mature yet, it has been relatively less studied so far. Since waveguide based multi-beam LOs have not been demonstrated at such a high frequency, the QCL [9] is the only practical solid-state source at 4.7 THz, which can provide multiple beams in combination with a phase grating. At present, given the power level and beam pattern of the current generation of THz QCLs suitable for use as an LO, such as third order DFB QCLs [10], they can typically only drive a single pixel superconducting hot electron bolometer (HEB) mixer. Progress, however, is rapid enough to overcome these issues soon with the next generation of 4.7 THz QCLs. One could think of using an array of QCLs instead. However, it is in general very challenging to produce multiple lasers with the same frequency. Furthermore, phase or frequency locking of multiple QCLs can be quite complicated.

No detailed study of a phase grating-based LO has so far been published beyond 1.4 THz [11], in which a FIR gas laser was applied. There are two challenges for such a system at higher frequencies. One is the realization of the phase grating since its surface finesse increases by the frequency and becomes more difficult to fabricate. The other is the 4.7 THz QCL with non-Gaussian beam and insufficient output power. Furthermore, the wave fronts of THz QCLs, which are not fully understood [12], might also affect the grating performance.

In this work we report an 8-pixel Fourier phase grating developed for operation at 4.7 THz together with its full characterization using a third order DFB QCL. In addition to the diffraction beam pattern and efficiency measurements, the power uniformity issue of such a LO array is discussed. We present an experiment of optically pumping an HEB mixer using one of the diffracted beams. The effects of the number of applied Fourier coefficients (FC) on the efficiency and also on the manufacturability of the grating are studied as well. We also demonstrate the grating bandwidth advantage using a FIR gas laser emission at 5.3 THz as the input.

2. Grating optimization and realization

A phase grating is formed by 2D repetition of a unit cell with a surface profile determined by the Fourier series based on a limited number of FCs, which modulates the phase of the incoming beam [6]. In addition to providing the required diffraction pattern and high efficiency, the unit cell profile has to have a minimum radius of curvature (MRC) meeting the manufacturing capability, beyond which the machine is not able to faithfully pattern. This minimum radius of curvature is limited by the diameter of available ball-end milling tools for fabrication via Computer Numerically Controlled (CNC) machining. Thus an optimization process needs to be performed. There are two main parameters for such an optimization. First is the number of applied FCs, which is proportional to the efficiency and inversely proportional to the MRC; second is the unit cell size, which is proportional to the MRC and inversely proportional to the divergence of the diffraction pattern.

Optics EXPRESS

The FCs for deriving the 2D profiles for beam multiplexing by 4 and 2 are calculated in MATLAB and optimised using a genetic algorithm to ensure the maximum achievable efficiency. They are then orthogonally superimposed to make the surface topology of the unit cell of an 8-pixel grating. The rectangular uniform arrangement of the diffracted beams requires the power to be distributed only among the 8 products of the diffraction orders of m = ± 1 and n = ± 3.

We use 13 FCs to simulate a 3x3 cm^2 grating, consisting of 25 times the unit cell of 1.2x1.2 mm^2 in two orthogonal directions, for operation at 4.7 THz with 25° incident angle with respect to the normal. A 3D drawing of 16 unit cells of the phase grating is shown in Fig. 1(a). We only show a part of the whole grating (225 unit cells), otherwise it would not allow a detailed view of the surface structure. Note that for clarity, the height is out of scale.

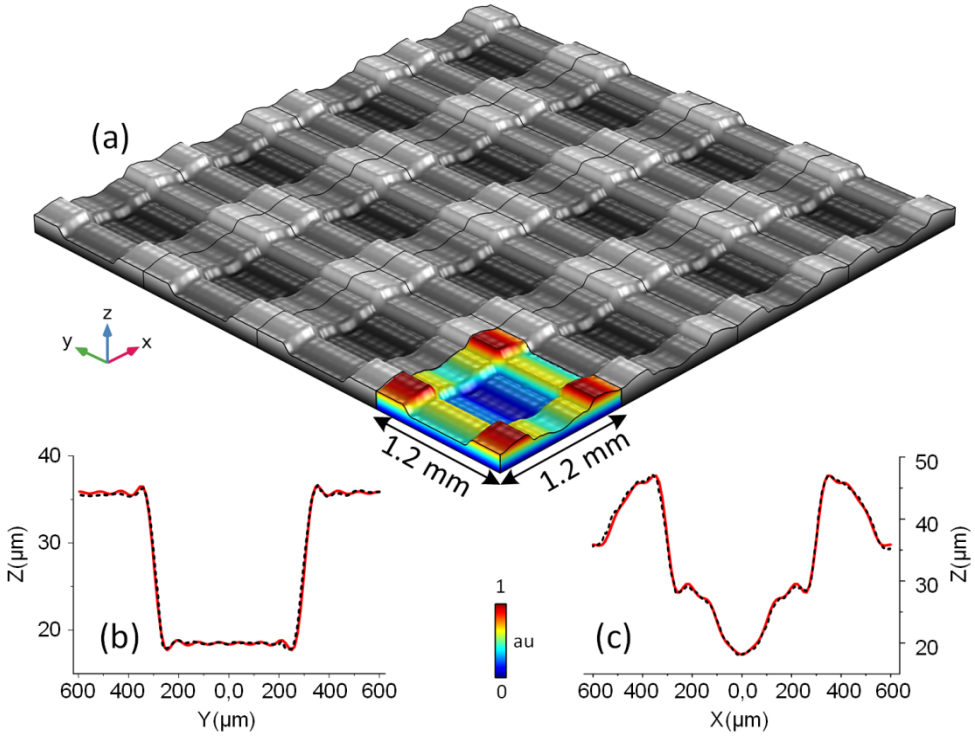

Fig. 1. (a) 3D drawing of 16 unit cells of the phase grating. A single unit cell is shown in colour. The height is out of scale for clarity, (b), (c) The calculated and manufactured 2D cross-section profiles of a unit cell. Z shows the height, and X and Y are the two lateral directions. The dashed black and solid red curves are the manufactured and calculated results respectively.

Based on the grating equation [13], $\sin\beta = \sin\alpha + m\lambda/\Lambda$, an angle of ~6° is expected between two adjacent diffracted beams, where α and β are the angles of incidence and the m'th (± 1 and ± 3) diffraction order respectively and Λ is the grating periodicity (equal to the unit cell size). The desired angle is chosen mainly based on the beam configuration of an existing HEB mixer array and its distance to the grating. This design results in an MRC of 112 μm, which is larger than the 90-μm radius of the ball end mill (available at the time we started) used with the KERN EVO micro-milling machine (at Arizona State University) that is employed for the grating manufacturing. In other words, the available machine is able to pattern all the fine surface structures. An aluminium plate (Aloca QC-10 Mold Alloy) is chosen as the grating material because of its very high reflectivity [14] and manufacturability. The manufactured 2D cross sections of a unit cell are measured by a Dektak XT30 stylus

Optics EXPRESS

profiler and plotted in Figs. 1(b) and 1(c) together with the calculated ones. They show very good matches with deviations in amplitude of < 1 μm.

3. Quantum cascade laser and the experimental setup

As the input source, we use a third order DFB QCL with an GaAs/AlGaAs active region based on four-well resonant phonon depopulation scheme [15]. It consists of 21 periods over a length of about 0.55 mm with 17-μm width and 10-μm thickness. Multiple lasers with a 7.5 GHz frequency spacing are grouped together on a single chip with a linear frequency coverage that allows targeting of a specific frequency. The active region was grown at Sandia National Laboratories by molecular beam epitaxy (MBE) while the QCLs were designed and fabricated at MIT. We choose a QCL with a single mode emission at 4.756 GHz mainly because of a relatively low water absorption in air at this frequency. The QCL was operated at a temperature of ~7 K using a pulse tube cooler. No power measurement was done for this specific QCL. However, based on the measured power of a similar laser on a different chip [16], we expect it to be around 0.25 mW.

A room temperature pyro-electric detector with an aperture diameter of 2 mm, mounted on a X-Y translational stage, is used for all the beam pattern measurements in this work. The QCL beam profile is measured in front of the cryostat window at a ~3 cm distance from the laser and plotted in Fig. 2(a).

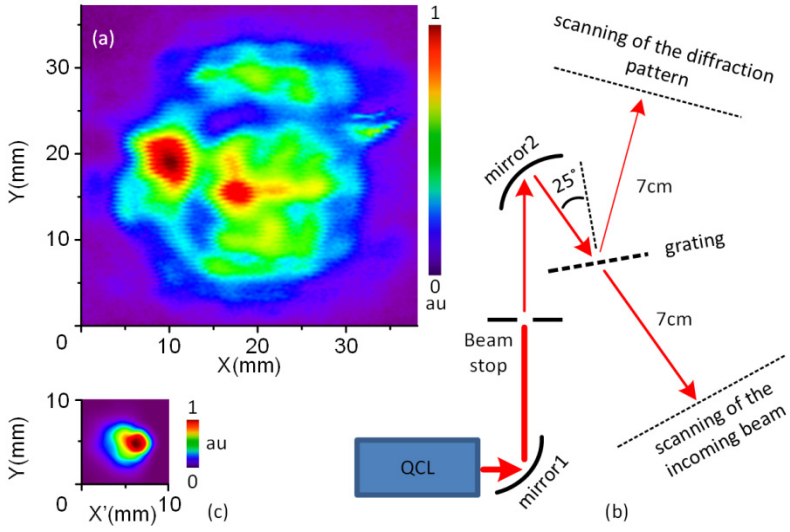

Fig. 2. (a) Quantum cascade laser beam pattern measured in front of the cryostat window, (b) Optical setup for collimation and filtering the laser beam. the line thickness is an indication of the intensity, (c) incoming collimated beam to the grating

The QCL beam is highly divergent with a strong deviation from a Gaussian profile. This QCL has the beam pattern that is worse than the others studied previously in our group [12,16]. Directly applying such a beam to the grating leads to the same order of divergence for the individual diffracted beams, which is more than their angular separation. This means that they are merged and would not be resolved from each other. Therefore we have introduced a spatial mode filter shown schematically in Fig. 2(b). Two parabolic mirrors are used for beam collimation. An iris beam stop in between the mirrors reduces the beam size by partially passing the left bright spot (and blocking the rest). This is the optimum setup we can make for this purpose regarding to the geometrical constraints. The resulted collimated beam shown in Fig. 2(c) then illuminates the grating at 25° incident angle with respect to the normal. For the reason to be explained in the next section, we measure the filtered beam at 7

Optics EXPRESS

cm away from the grating position when it is removed. The aperture size of the beam stop is adjusted to maximize the passing QCL power whilst still resolving separated diffracted beams at a reasonable distance from the grating. By integrating the intensity of the beam patterns and considering about 1.4 and 0.5 dB absorption losses by the cryostat UHMW-PE window and the air respectively, we find that about 78% of the total QCL power in the whole beam pattern is blocked by this setup. This large power waste already explains the crucial role of the laser beam pattern. If the latter was more concentrated in a small area, a much smaller (or no) portion would be needed to be removed.

4. Measurement and simulation results

Since the grating unit cell has two different orthogonal cross-sections, it results in two different diffraction beam patterns (either 4 by 2 or 2 by 4) when illuminated from each orthogonal direction [11]. The beam patterns measured at a distance of 7 cm from the grating using the setup shown in Fig. 2(b), for both cases are plotted in Fig. 3. The high-resolution patterns have been achieved by fine scanning with a step size of 0.1 mm. We measure the incoming beam in the same distance from the (removed) grating to cancel out the effect of the air absorption in the efficiency calculations later on. As expected, all diffracted beams copy the incoming beam profile, but horizontally flipped. The predicted ~6° angular distance between each two adjacent beams is experimentally confirmed. The unwanted higher diffraction orders are visible around the desired ones with much weaker intensities. This gives a good visual feeling of the efficiency. Since both diffraction patterns show a similar behaviour in terms of power and spatial distribution, we focus on the result shown on the left side (4x2) in the rest of the paper.

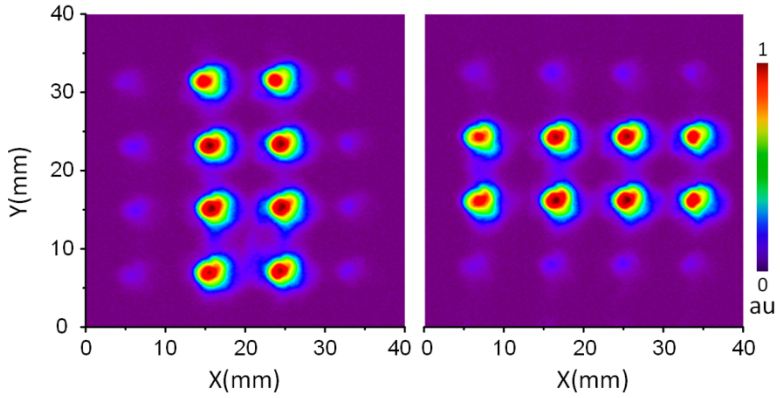

Fig. 3. Measured diffraction patterns of the grating at 4.7 THz using a quantum cascade laser with 25° of incidence in two different orthogonal directions.

For estimating the efficiency, we take the ratio between the integrated intensities of all the desired diffracted beams and the one of the incoming beam. It should be mentioned that the noise floor of the room temperature detector, which can affect the efficiency analysis, is removed before the integration. We find an efficiency of 74.3%, which is close to 75.4% predicted by a 3D simulation using the RF module of COMSOL. The latter is done by importing the grating surface profile and simulating a periodic port with periodic boundary conditions. Extracting the S parameters of the port then gives the efficiency. The maximal grating efficiency is dependent on the diffraction pattern. So the 75.4% efficiency is associated with our prerequisite 4x2 rectangular beam configuration, otherwise the efficiency can be different.

We analyse the uniformity of the power distribution among the diffracted beams by applying the same method of integrating the intensity. The fractions of the incoming beam

Optics EXPRESS

power distributed to the diffracted beams shown on the left side of the Fig. 3 from top to bottom of the left column are 9%, 10.4%, 9.5%, and 8.6% and on the right column are 8.6%, 10.3%, 9.3% and 8.4%. The power in the individual beams varies within ~21% around its average value. The 3D simulation also shows that the intensities of the four central beams are slightly higher to the same extent.

In order to confirm that such a power variation among the diffracted beams may not deteriorate the performance of an HEB array, in which all the HEBs require the same LO power, we use our existing experimental data to evaluate the effect of the LO power tolerance to the sensitivity of a single mixer. This particular measurement was done at 4.3 THz (very close to our frequency of interest). The receiver noise temperature (T_{rec}) of the HEB mixer was measured as a function of LO power, reflected by the HEB current (inversely proportional to the LO power) at a constant bias voltage of 0.8 mV. The result is shown in the inset of Fig. 4 and suggests the optimum current of ~38 μA, in which the T_{rec} becomes minimal [17]. The correspondence between the current and the LO power can be estimated from the pumped current-voltage (I-V) characteristics by using the isothermal technique [18]. The multiple I-V curves, measured at different LO powers, are plotted in Fig. 4, where the top curve (in brown) is recorded without LO (superconducting state) and the bottom (in red) with a sufficiently high LO power to fully pump the device (to the resistive state). By estimating all the LO powers and their corresponding T_{rec}s we find that the change in the T_{rec} is less than 4% when the LO power varies within about 21%. We therefore conclude that despite the power variation (~21%), the multi-beam LO made by our phase grating can pump a uniform HEB array without affecting the uniformity of the T_{rec}.

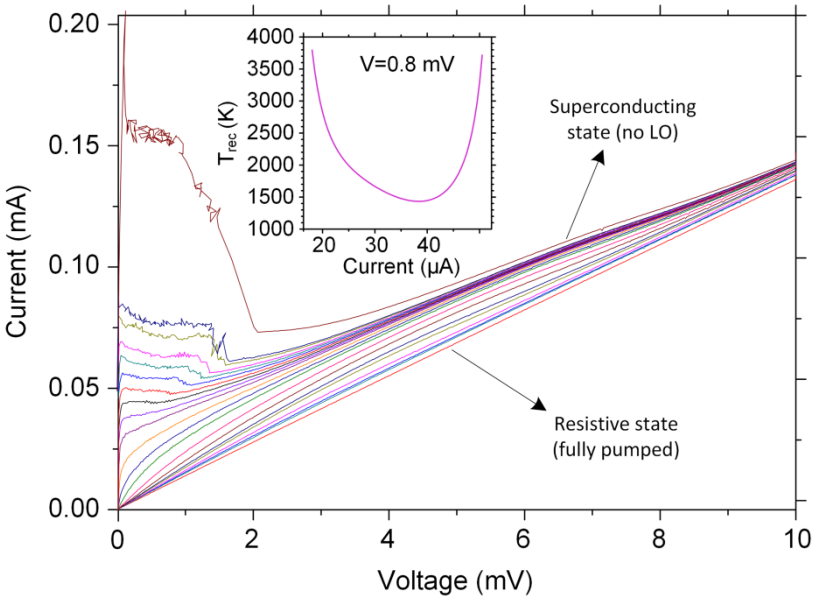

Fig. 4. The current-voltage characteristics of the HEB mixer at different levels of the LO power, which is zero in the top curve (in brown) and sufficient to fully pump the device in the bottom curve (in red). Inset: Measured receiver noise temperature (T_{rec}) of a hot electron bolometer (HEB) mixer versus the current at a bias voltage of 0.8 mV. The current is inversely proportional to the absorbed local oscillator (LO) power.

We study the effect of the number of applied FCs on the grating efficiency and manufacturability using the same 3D simulation. The results, which are plotted in Fig. 5(a), show that decreasing this factor from 13 to 6 degrades the efficiency from 75.4 to 69% (by ~6%) while increases the MRC by ~274 μm (~300%). As explained before, the MRC determines the manufacturing requirement, which is the size of the ball end mill in our case.

Optics EXPRESS

This is an interesting and useful finding since one can ease the manufacturing considerably by sacrificing a few percent of the efficiency. 3D surface profiles of the resulting unit cells from applying 6 and 13 FCs are plotted in Figs. 5(b) and 5(c), respectively, illustrating the effect on the surface fines and challenge of the manufacturing.

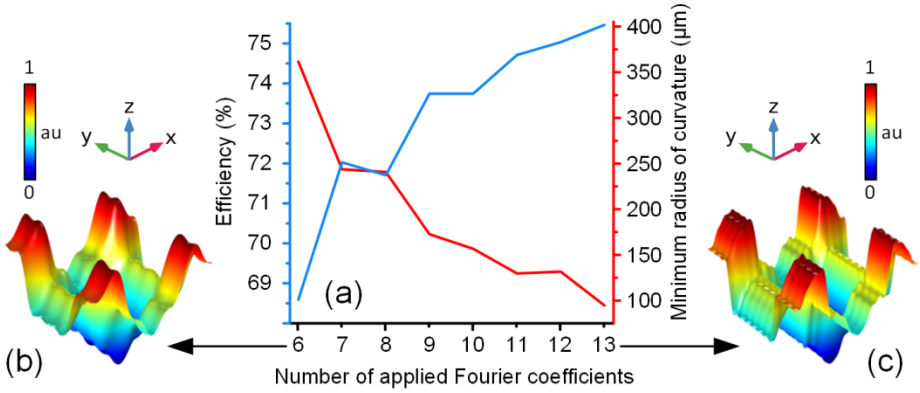

Fig. 5. (a) Grating efficiency and the surface minimum radius of curvature (MRC), versus the number of applied Fourier coefficients (FCs) in design, (b), (c) 3D profiles of the unit cells made by 6 and 13 FCs, respectively.

5. Grating operation bandwidth

The bandwidth of a phase grating is an interesting property, which has so far been less explored. In theory, it can perform well over a wide frequency band by properly changing the incident angle. A grating designed for the frequency f with an incident angle θ with respect to the normal works with the same efficiency as long as the value of $f \times \cos(\theta)$ is fixed. In our case, if we consider an applicable range of 0 to 45 degrees for the incident angle, the grating can function optimally from 4.3 to 6 THz.

Due to the limited available THz sources, we verify the performance of the 4.7 THz grating using a FIR gas laser line at 5.3 THz. The measured incident beam and the resulting diffraction pattern at 15 cm away from the grating are plotted in Fig. 6.

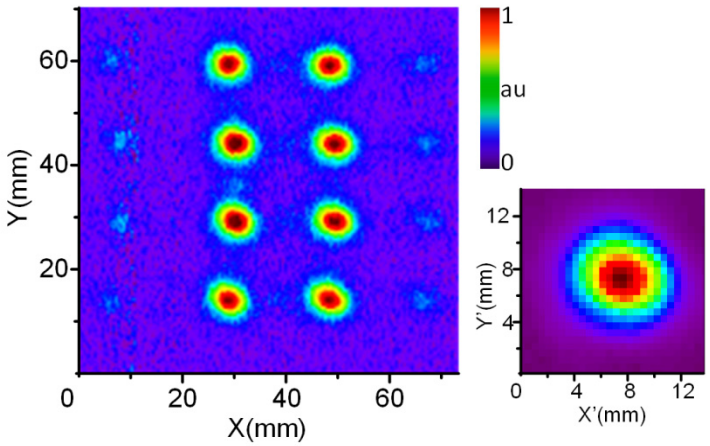

Fig. 6. Diffraction beam pattern measured at a distance of 15 cm from the grating (left) and the incident beam (right) at 5.3 THz measured using a FIR gas laser.

In this particular measurement, the incident angle is chosen to be 37° (as opposed to 25° for 4.7 THz). The diffracted beams are in the same order of spatial and power distributions as

Optics EXPRESS

the case of 4.7 THz described earlier in this paper. The derived efficiency by applying the same analysing method is 74%, being almost equal to the 4.7 THz case. Our measurement at 5.3 THz, being 0.6 THz higher than the targeted frequency, confirms that the grating bandwidth should be more than 13%. The broadband grating characteristic offers a potential for other applications including multiple imaging at different frequencies using a single grating [19].

6. Pumping a superconducting HEB mixer

To further quantify the performance of the 4.7 THz grating, we perform an experiment, in which we apply one of the eight diffracted beams (originated from the QCL) as the LO to pump a superconducting HEB mixer. We have to change the optical setup in order to redirect the diffracted beams towards a suitable place for putting and manually fine positioning a bulky liquid helium cryostat, in which the HEB is mounted. By doing so and considering the very limited geometrical flexibility, we could illuminate the grating with only about 9 μW. An additional beam stop is introduced after the grating to pick only one, out of the eight diffracted beams. Then it is coupled into a quasi-optical (lens-spiral antenna) HEB mixer using a focusing lens. We succeed in coupling ~50 nW to the HEB mixer, which is derived from the pumped I-V characteristics using the isothermal technique [18]. By taking into account the total optical loss of ~32.6 dB [20] in the entire system, we find that ~91 μW of the QCL power is used (we assume that the QCL has a 0.25 mW output power). We think this power fraction is reasonable by attributing the difference to the partial mismatch between the non-Gaussian LO beam and beam of the HEB mixer, and also to the uncertainty in the actual QCL output power.

Let us now estimate the required QCL power for a practical 8-pixel array with spiral antenna coupled HEB mixers. To do so, we consider the system as the following; a) each mixer needs a pumping power of 220 nW; b) Si lens for the mixer has an antireflection (AR) coating at 4.7 THz; c) a 3 μm thick Mylar beam splitter is used for a heterodyne measurement; d) the setup is in vacuum; e) the focusing lens is made of silicon with double sided AR coating at 4.7 THz; f) The QCL has an ideal Gaussian beam. This system has an optical loss of ~26.2 dB [21], implying that a power of ~92 μW from the QCL is needed in this case. However, the fraction of the power in the beam in the fundamental Gaussian mode can be much less (e.g. 10%) in practice, which increases the required QCL output power considerably (e.g. 0.9 mW). It is worth to mention that producing THz QCLs with either higher power or improved beam profile seems to be feasible [22,23] considering the rapid progress being made in the community.

7. Conclusions

We report for the first time a Fourier phase grating for generating eight local oscillator beams using a single mode 4.7 THz DFB quantum cascade laser as the input source. We characterized the grating performance by measuring the diffraction pattern and deriving the diffraction efficiency of 74.3%, which is in an excellent agreement to the 3D simulation result. We demonstrated that the power uniformity of such a multi beam LO is sufficient, leading to uniform sensitivities of the array mixers. The effects of applying different number of Fourier coefficients in simulation, on the efficiency and manufacturing is discussed. The broad-band characteristic of the grating is verified by its evaluation at 5.3 THz, where we found the same performance as the case for 4.7 THz. Finally we analysed the power issue by coupling one of the diffracted beams generated by the QCL-grating combination to a superconducting hot electron bolometer mixer. We estimate that an 8-pixel array receiver, in which each mixer needs a power of 220 nW, requires from 92 μW to 0.9 mW for the QCL power if its Gaussian component has a power fraction from 100 to 10%.

Our work demonstrates the principle of a novel array local oscillator technology, which is demanded for future space missions. It is a prototype LO unit for a NASA science mission

Optics EXPRESS

GUSTO (Galactic/X-galactic Ultra-duration-balloon Spectroscopic/Stratospheric Terahertz Observatory), which is scheduled to launch in 2021 from Antarctica and map three THz fine structured lines including [OI] using an 8-pixel receiver array.

Funding

U.S. Department of Energy's National Nuclear Security Administration (DE-NA-0003525).

Acknowledgments

One of the authors (B. M.) acknowledges the support and encouragement from Leo Kouwenhoven. We also acknowledge useful discussions with Chris Walker, Kobus Kuipers, Paul Urbach, and Akira Endo. The authors would like to thank Yuchen Luo for making his grating codes available for this work, Matt Underhill for fabricating the gratings and David Thoen for helping with the surface profile measurements. EU RadioNet and TU Delft Space Institute are acknowledged for their supports. The work at MIT was supported by NASA. The work at Sandia was performed, in part, at the Center for Integrated Nanotechnologies, an Office of Science User Facility operated for the U.S. Department of Energy (DOE) Office of Science. Sandia National Laboratories is a multimission laboratory managed and operated by National Technology and Engineering Solutions of Sandia, LLC., a wholly owned subsidiary of Honeywell International, Inc., for the U.S. Department of Energy's National Nuclear Security Administration.